Extension, Displacement, and Block Rotation in the Larger Gullfaks Area, Northern North Sea: Determined from Map View Restoration[1]

Delphine Rouby,[2] Haakon Fossen,[3] and Peter R. Cobbold[2]

ABSTRACT

Numerical map view restoration of the larger Gullfaks area on the western side of the Viking Graben reveals a Late Jurassic apparent displacement field that is slightly divergent, with displacement vectors trending east-northeast–west-southwest to east-southeast–west-northwest. The predominant extension direction is east-west in the Gullfaks field, changing to east-southeast-west-southwest in the Gullfaks Sør area. We relate the divergent pattern to extensional collapse over low-angle extensional detachments in the eastern part of the area. The detachments also explain the anomalously high extensions in this same area. Total extension in the horizontal plane is estimated to be 19% on average in the larger Gullfaks area, whereas it is 42 and 33% in Gullfaks and Gullfaks Sør, respectively. Block rotations (about vertical axes) are minor (mostly <5°). Calculated fault-slip directions indicate that major north-south–striking faults are mostly dip-slip, whereas accommodation faults or transfer faults, oriented at high angles to the major faults, tend to be oblique slip.

In general, numerical or manual map view restoration is useful before choosing and balancing vertical sections. In most of the Gullfaks area, strain is close enough to plane strain and block rotations are small enough for section balancing to be reliable. East-west sections should be chosen across the main Gullfaks field, and east-southeast–west-northwest sections in the Gullfaks Sør area.

[1]Manuscript received April 10, 1995; revised manuscript received November 7, 1995; final acceptance February 12, 1996.

[2]Geosciences Rennes (CNRS), Universite de Rennes, 35042 Rennes Cedex, France.

[3]Statoil, GF/PETEK-GEO, N-5020 Bergen, Norway.

We thank Statoil, Norsk Hydro a.s., and Saga Petroleum a.s. for permission to publish these results. J. Hesthammer is thanked for suggesting improvements on an early version of the paper. The Statoil maps applied in this study are based on seismic interpretations by I. Firth, H. Fossen, R. Hansen, J. Henden, J. Hesthammer, O. Lyse, S. Løkkebø, L. K. Strønen, and A. Thon.

INTRODUCTION

The Gullfaks area is located on the western margin of the Viking Graben of the North Sea rift system (Figure 1). Because of its position in the economically most important area of the North Sea, this area's structural geology has attracted much interest over the last decade (Fossen, 1989; Petterson et al., 1990; Koestler et al., 1992; Fossen and Hesthammer, 1994; Færseth et al., 1995; Fossen and Rørnes, 1996). The area also contains the highest density of geologic data in the North Sea rift system, including a large amount of 3-D (three-dimensional) seismic surveys, deep seismic profiles, and dipmeter data, in addition to cores and other information from about 150 exploration and production wells. The large and still-growing amount of data makes the area well suited for detailed structural analysis to understand upper crustal extensional deformation in rift systems. In this paper, we use Statoil's detailed maps of the Gullfaks and Gullfaks Sør fault blocks to restore the area in map view. Restoration is performed using the numerical restoration method described in Rouby et al. (1993) and Rouby (1995). This method describes displacement patterns and quantification of displacements, rotations, and extensions associated with rifting. The method is also useful for validating structural interpretations, although this is not the object of this paper.

GEOLOGIC SETTING

The Viking Graben (Figure 1, inset) is a large north-south–trending graben that originated during the Permian–Triassic phase of extension of the North Sea (e.g., Roberts et al., 1990, 1995). However, the largest Permian–Triassic extension appears to have occurred east of the present Viking Graben, which developed into a distinct graben system only during the Late Jurassic (Gabrielsen et al., 1990; Roberts et al., 1995). Subsidence occurred throughout the Triassic,

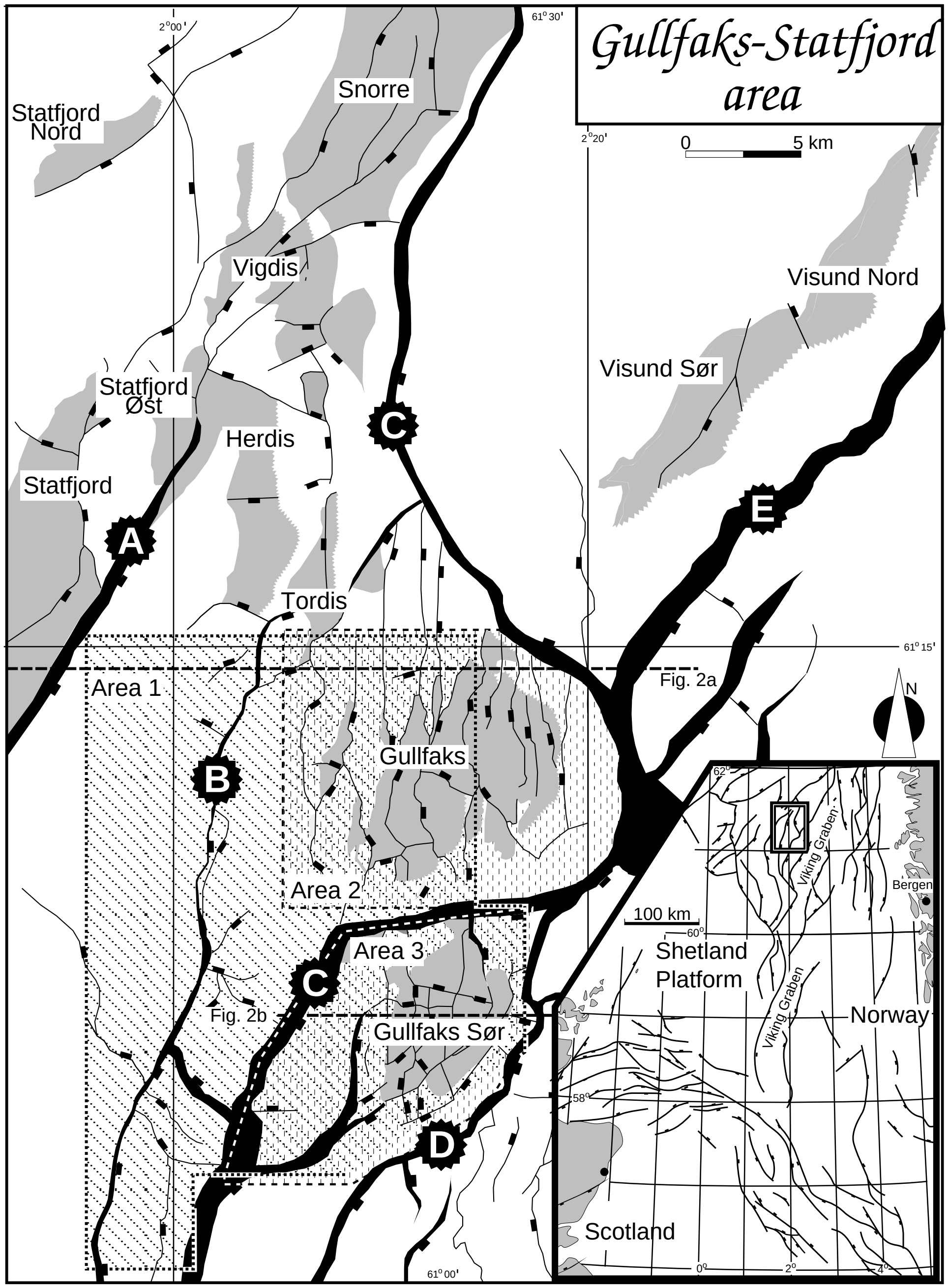

Figure 1—Location of the Gullfaks-Statfjord area in the northern North Sea. First-order faults are marked as wide, black separations, and second-order faults as thinner lines. Boxes indicate the three areas subjected to restoration (areas 1, 2, and 3). The names of the main fields and prospects in the area are indicated (shading), and the main faults are named A–E.

when 3000 m of Triassic sediments were deposited in the northern Viking Graben. A major uplift (erosion) is recorded in the Lower–Middle Jurassic series of the central North Sea, where a major rift dome was located. In the northern Viking Graben, doming-related regression led to the deposition of the Brent Group sandstones. The rate of crustal extension appears to have increased substantially from the Middle into the Late Jurassic. The Shetland Platform was uplifted, and differential fault block subsidence was associated with the development and the rotation of large fault blocks. The effects of this Late Jurassic phase are very pronounced on seismic data and of greatest importance for the oil industry.

The rate of extension decreased in the Early Cretaceous. Thermal subsidence appears to have influenced the entire North Sea until the Paleocene. A general rise in sea level resulted in progressive overstepping of the platform and burial of Jurassic fault blocks during the Cretaceous (e.g., Ziegler, 1990).

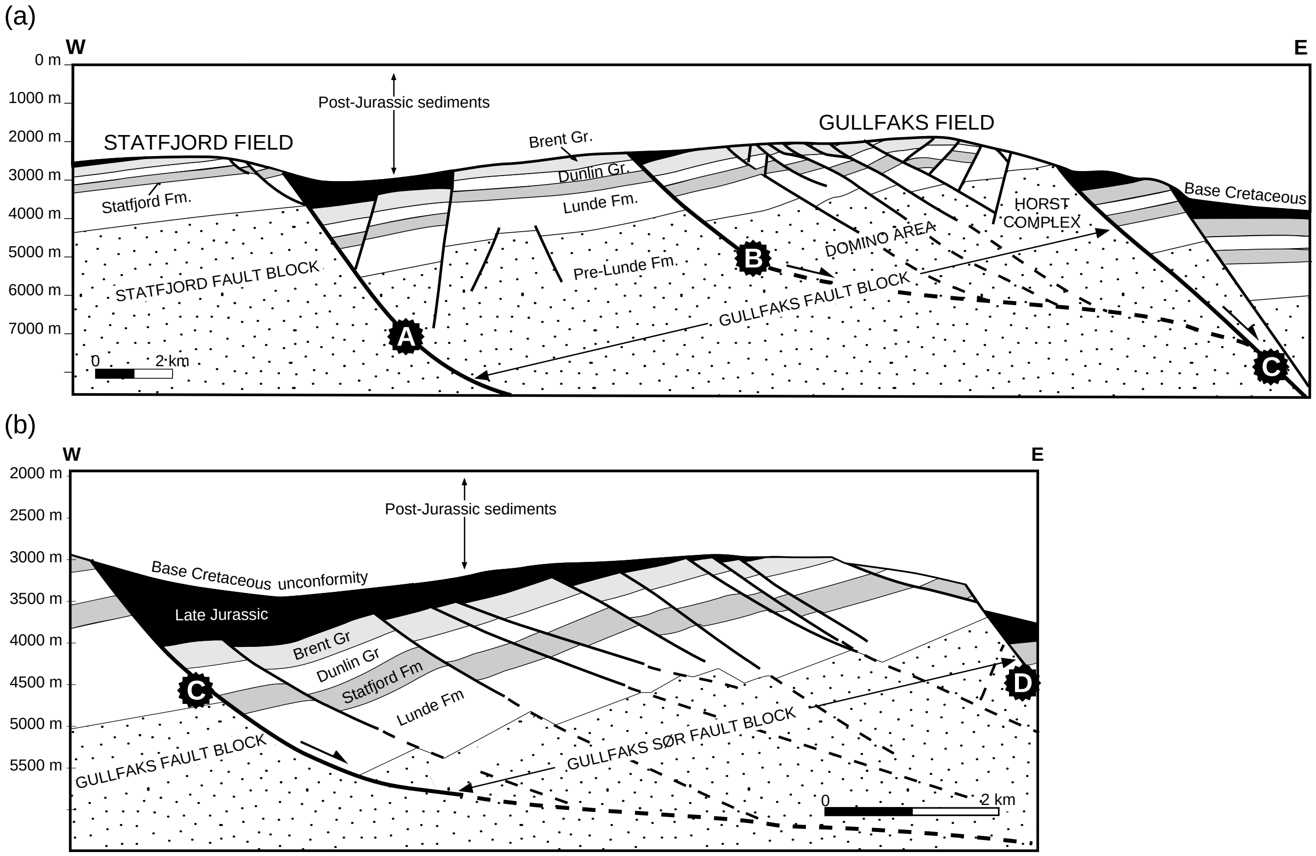

Figure 2—(a) East-west depth profile through the northern part of the Gullfaks fault block. (b) Profile through the Gullfaks Sør fault block. No vertical exaggeration, but note difference in scale between (a) and (b). Faults are dashed where the seismic resolution is poor. See Figure 1 for location.

Structural Setting

The Gullfaks oil field (Sæland and Simpson, 1982; Karlsson, 1986; Erichsen et al., 1987; Petterson et al., 1990) occupies the eastern part of a first-order fault block (the Gullfaks fault block) in the North Sea (bounded by faults A and C in Figures 1 and 2a). First-order normal faults (with kilometer-scale displacements) separate the Gullfaks fault block from the Statfjord fault block to the west and the graben area to the east. The easternmost fault is strongly non-planar, and wraps around the Gullfaks field. To the south, this eastern first-order fault splits into two branches, defining the Gullfaks Sør fault block (defined by faults C and D in Figures 1 and 2b).

Stratigraphy

Within the Gullfaks area, the sedimentary sequence consists of Triassic continental sandstones and shales (Lunde Formation) overlain by latest Triassic to earliest Jurassic alluvial sandstones of the Statfjord Formation and marine claystones, regressive sandstones, and marine shales of the Dunlin Group (Figure 2). The Middle Jurassic sandstones of the Brent Group constitute a regressive-transgressive sequence. The base Cretaceous unconformity represents a time gap of up to 100 m.y., and Cretaceous shales form the cap rock to the Gullfaks field. Late Jurassic sediments (black in Figure 2) have locally been preserved within tilted fault blocks. The Cook Formation, Statfjord Formation, and Brent Group constitute the main reservoirs in the area. In Gullfaks field, the total recoverable reserves are estimated to 280 million standard m^3 of oil and 25 billion standard m^3 of associated gas. The similar numbers for Gullfaks Sør are approximately 40 million standard m^3 of oil and 60 billion standard m^3 of associated gas.

Gullfaks Fault Block

The western part of the Gullfaks fault block is characterized by relatively few faults. Faulting is more pronounced toward the central and eastern part of the Gullfaks fault block, known as the Gullfaks field. The structural geology of the Gullfaks field has been treated in detail by Fossen and Hesthammer (1994). The field is divided into a large western domain, where fault blocks exhibit a domino-style geometry, and an eastern elevated and deeply eroded horst complex (Figure 2a). Between these areas is a zone that accommodated the differences in deformation between these two subareas. In the domino area the Jurassic beds exhibit an average dip of about 15° toward the west, whereas the faults are dipping 25–30° toward the east. The bedding is somewhat steeper (~20°) in the footwalls of the domino blocks than in their hanging wall, where it locally becomes horizontal. In the horst complex, layering is subhorizontal or gently westward dipping, and faults are much steeper (60–70°). Recent reprocessing of deep seismic lines across the Gullfaks block (T. Odinsen, 1995, personal communication) indicates the presence of a shallow eastward-dipping detachment under the Gullfaks field (Figure 2a, dashed line).

The horst area balances relatively easily by rigid block rotations about horizontal axes, whereas in the domino area rigid block rotations predict relatively shallowly (45°) dipping faults at the onset of deformation. Physical experiments, seismic data, and field observations suggest most normal faults initiate with dips of at least 60° (Anderson, 1951; Jackson, 1987), and commonly as high as 70° (Walsh and Watterson, 1988). We therefore suspect that the domino faults formed with an initial dip of at least 60°, which implies a certain amount of internal deformation in the domino blocks. The nonplanar geometry of the bedding is further evidence for internal block deformation, and from geometrical reasoning (Fossen and Hesthammer, in press), the internal deformation may be modeled in simple terms as a shear synthetic to, but steeper than, the domino faults.

Gullfaks Sør Fault Block

The Gullfaks Sør fault block forms the hanging wall to a major, listric normal fault (fault C, Figure 2b). The hanging-wall deformation is accommodated by domino-style faulting. Faults dip 25–30° to the east and sedimentary layers dip about 15° to the west; i.e., a geometry very similar to the domino system in the Gullfaks field. Hence, the discussion on distributed deformation in the domino system of the Gullfaks field also applies to the Gullfaks Sør block.

METHOD OF RESTORATION

Principle

We use a numerical method for restoration in map view of the study area. A full description of the method can be found in Rouby et al. (1993) and Rouby (1995). We here briefly describe the principle and the main assumptions.

The method seeks to reconstruct the original undeformed state of a given interpreted seismic horizon currently truncated and dismembered by a population of normal faults. In effect, we seek to close the fault gaps that appear on a fault heave map with a minimum of overlap and remaining gaps. The input data are maps of stratigraphic horizons displaying the fault network and thus the horizontal component of dip-slip displacement (heave) across each fault. The fault heave maps are obtained by vertical projection of hanging wall and footwall cutoff onto a horizontal plane.

Assumptions

We consider a horizon to be perfectly restored when all fault gaps are closed. To close them, our method relies on three assumptions. (1) The fault pattern is completely divided into a finite number of fault-bounded blocks. This pattern must be defined before fault gaps are closed. (2) Blocks are assumed to be rigid or deformed internally by vertical shear (Figure 3) so that fitting involves only translations and rigid block rotations about vertical axes. (3) Restoration in map view does not restore the component of displacement related to rigid tilting about horizontal axes, folding, or distributed small-scale ("ductile") deformation different from vertical shear. As discussed, there are reasons to believe that inclined shear models the internal deformation better than vertical shear; however, in either case the model is a simplification of the actual deformation pattern within the fault blocks. Although it introduces a qualitative error to the restoration, internal block deformation, with few exceptions, is subordinate to the seismically resolvable deformation (e.g., Westaway, 1994), and the main characteristics of the deformation can still be investigated by the restoration procedure outlined in this paper.

Preliminary Data Processing

From the fault heave map (Figure 4a) we produce a modified map showing an assembly of fault-bounded blocks. To do so, we extrapolate fault

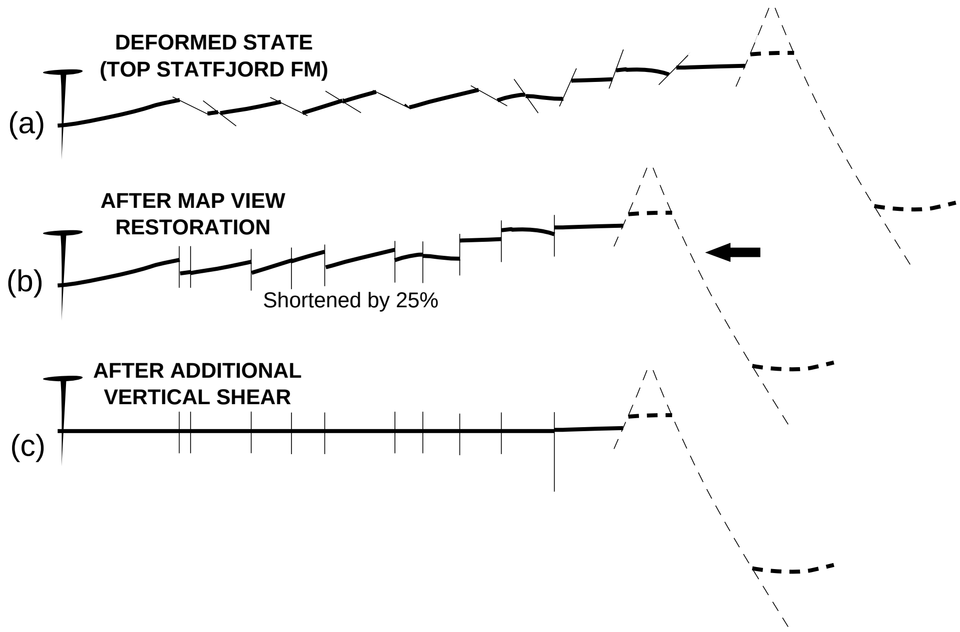

Figure 3—(a) Profile through the faulted Statfjord Formation, Gullfaks field. The Statfjord is reconstructed in the eroded eastern part of the horst complex. (b) The effect of map view restoration. Application of vertical shear to obtain a continuous horizontal layering (c) has no influence on the map pattern.

traces until they intersect (Figure 4b). Large and elongated blocks also may be subdivided using artificial boundaries to allow for some internal deformation to take place. Such artificial boundaries are straight lines perpendicular to the faults. The result is a map where blocks are entirely surrounded by faults (Figure 4c).

Numerical Restoration Procedure

We assume that a horizon is restored when fault heave gaps are closed. One or more stationary blocks are chosen (block 1 in Figure 4c), and the least mean squares procedure closes the gaps by packing blocks against stationary blocks (Figure 4d). The basin margin or a large block at the edge of the study area is normally chosen as the stationary block. The best fit is assumed to be obtained when the distances between neighboring blocks are minimized, which generates a set of equations in terms of the unknown block transitions and rotations.

Finite Deformation

From the deformed and restored states, we calculate the finite horizontal displacement field for each horizon, amounts of bulk extension in the horizontal plane, and surface dilation (Figure 4e). The displacement vectors connect grid points in the deformed state (Figure 4c) and restored state (Figure 4d), and therefore are displacement vectors for the total deformation. The vectors can therefore be considered as the sum of the successive displacement events in the area. The length of the displacement vectors thus increases away from the stationary block. Finite slip directions on each fault can also be deduced from the relative movements of block boundaries.

RESTORATION OF THE TOP BRENT HORIZON, LARGER GULLFAKS AREA

To obtain a regional displacement pattern, we restored a map of the top Brent horizon covering area 1 in Figure 1. The map is a compilation of several of Statoil's 3-D seismic interpretations, consisting of one for the northeastern part of the area (the Gullfaks field), one for the southeastern part of the area (the Gullfaks Sør structure), and one for the whole western part of the area.

Fault Block Map and Restoration

The fault heave map is shown in Figure 5a, and includes a first-order fault separating the main eroded Gullfaks field from the Gullfaks Sør structure to the south. This first-order fault shows more than 1 km of heave. Second-order faults (typically with a few hundred meters of heave) strike north-south in the northern part of the area and north-northeast–south-southwest in the southern part (Figure 5a). Third-order faults (characterized by 10–100 m of heave) occur throughout the area, and

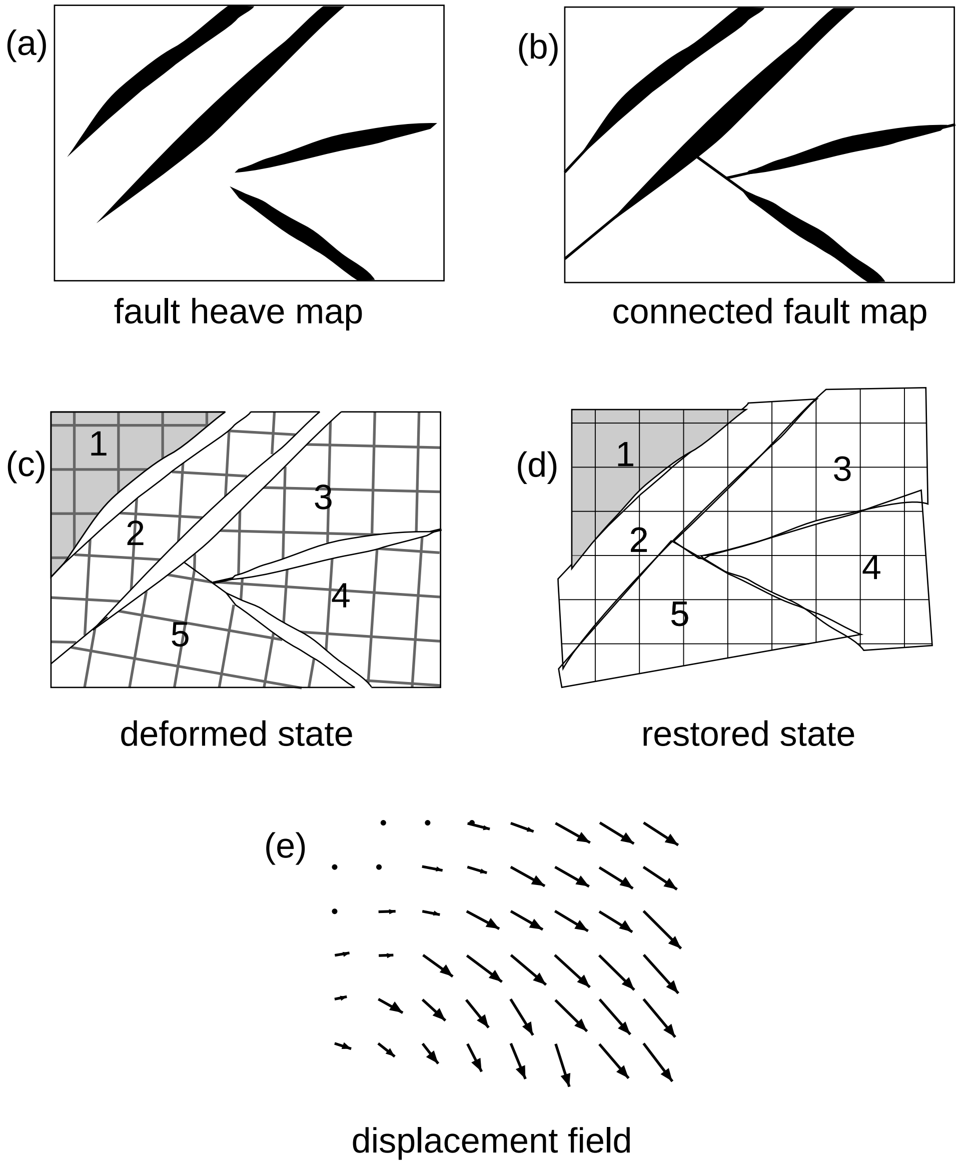

Figure 4—Method of restoration. From the initial fault heave map (a) fault traces are extrapolated to construct a map where the fault blocks are entirely surrounded by faults (b). Fault blocks are numbered, and a stationary block (block 1) is chosen (c). Restoration is performed by packing blocks against the stationary block (d). From the restored and deformed states we compute the finite displacement field (e). Each vector connects corresponding points of a material grid on the restored and deformed maps (c, d). The vectors thus represent the total deformation, and give no information about the deformation history (intermediate stages).

cover the full range in orientation from north-south to east-west.

By extending some of the fault tips and adding a few minor faults to the fault heave map, we defined 129 blocks entirely surrounded by faults (Figure 5a). Because the fault pattern is quite coalescent (interconnected), only large and elongated blocks were subdivided by addition of artificial straight boundaries. The part of the area closest to the rift margin was chosen as the stationary block (gray area, Figure 5a). All other external boundaries are free.

Application of the numerical procedure to the original block map yields a restored map where gaps and overlaps are minimized (Figure 5b). Some local gaps and overlaps do remain, for example, in the northwestern part of Gullfaks Sør or west of Gullfaks Sør. Gaps and overlaps can be attributed to either internal block strain or erroneous interpretation of seismic data. The dashed line in Figure 5b indicates the present-day shape of the area. The area of the deformed (present) state is 119% of the undeformed (restored) area. Hence, the dilation or total extension in the horizontal plane is estimated to be 19%. The extension in the east-west direction ranges from about 10% (1.25–1.8 km) in the northern part to 17% (2.5 km) in the central portion to approximately 8% (0.9 km) farther south (as measured from the gray, stable block to the eastern limit of the area shown in Figure 5). The higher east-west extensions in the central portion of the deformed area are related to the contribution from the Gullfaks Sør block.

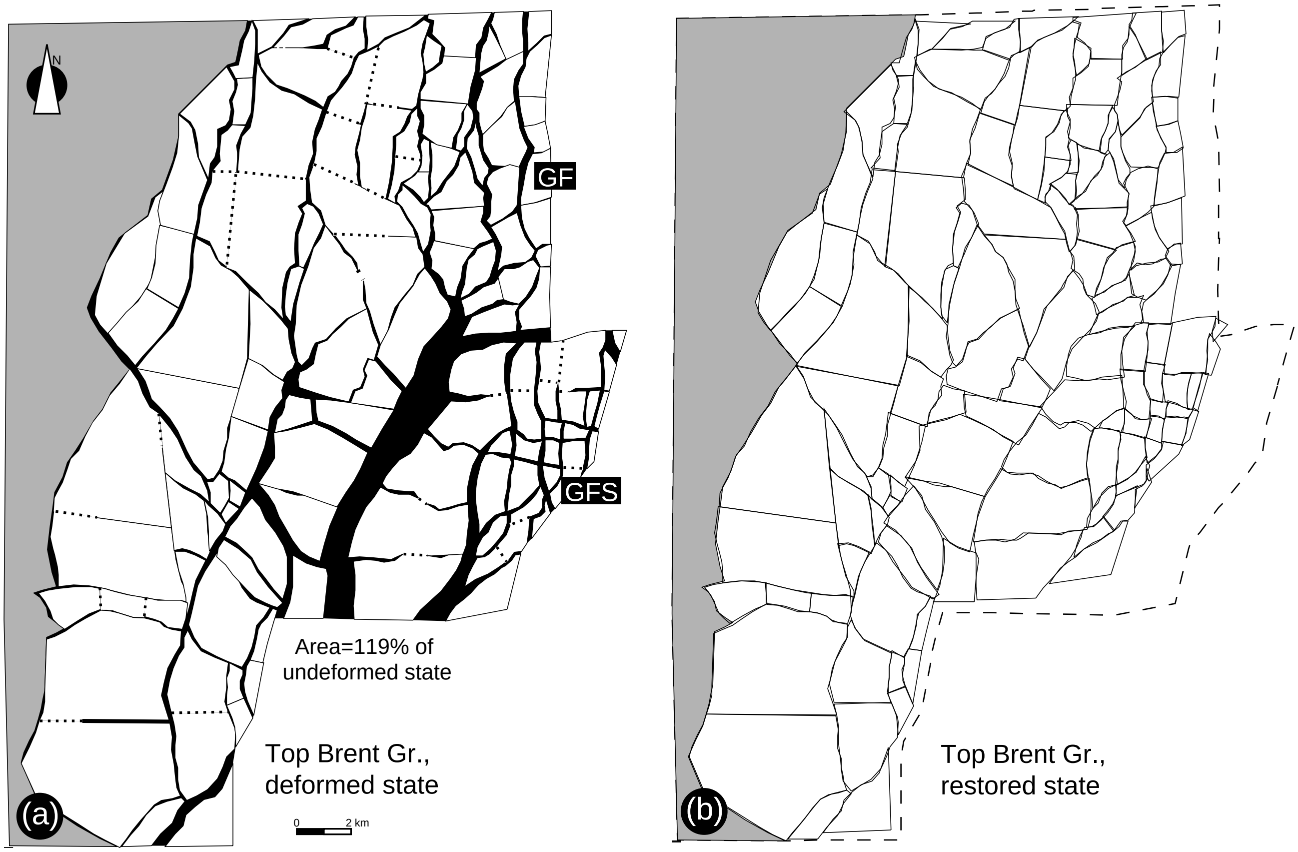

Figure 5—Fault block maps for (a) the current state and (b) the restored state for the top Brent Group (area 1, Figure 1). Extended (artificial) faults or portions of faults are marked as dashed lines. Shaded area indicates the chosen stationary block. Unshaded blocks are packed against the stationary block to the point where gaps and overlaps have been minimized. Dashed line outside the restored area indicates the present outline of the study area. GF = Gullfaks field, GFS = Gullfaks Sør structure.

Fields of Finite Displacements and Rotations

The field of finite displacement (Figure 6a) shows vectors ranging from northeast-southwest to southeast-northwest. Several subdomains of differing displacement directions can be identified: a northern domain of northeast-southwest displacements, a northeastern domain of almost east-west displacements, a southern domain of southeast-northwest displacements, and a southeastern domain of larger east-southeast–west-northwest displacements. This latter domain covers the Gullfaks Sør fault block. This part of the displacement field is strongly influenced by slip on the first-order fault separating the Gullfaks and Gullfaks Sør fault blocks. The vector field is slightly divergent also within the Gullfaks Sør fault block. In general, the displacement field suggests a nonplane strain at the scale of the larger Gullfaks area.

The block rotation map shows the amount of rigid rotation of each block (rotation about a vertical axis through the center of the block) between the restored and the deformed state (Figure 6b). We have distinguished between clockwise and counterclockwise rotations. Rotations are relatively small (most are between –5 and 3°). We found no general pattern to the distribution of sense or magnitude of rotation within the area, suggesting that most of the computed rotations are related to local displacement gradients along the strike of the faults.

Directions of Slip on Faults

Directions of slip on faults, as deduced from restoration, are shown in Figure 7. A considerable variation in slip directions is seen throughout the area. Many faults are dip-slip or close to dip-slip, but there are also a number of exceptions. For example, the southwestern part of the area contains some north-south–striking faults with

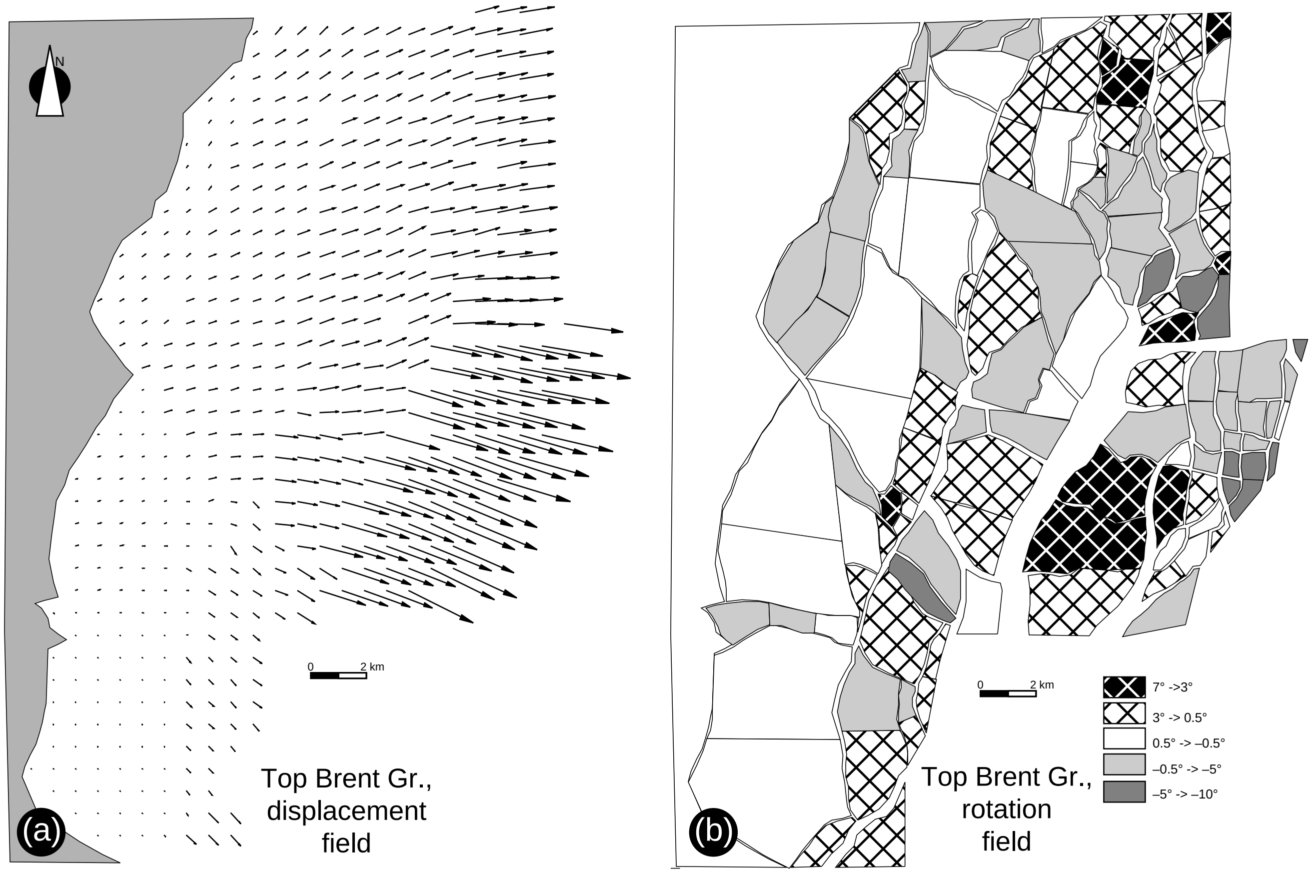

Figure 6—(a) Field of finite displacements for the top Brent horizon (area 1 in Figure 1). Each vector spans the distance between corresponding points in the restored and deformed states. (b) Field of finite block rotations for the same area. Each block is shaded according to its sense and magnitude of rotation between the restored and deformed states. Key shows magnitude (in degrees), with positive numbers indicating counterclockwise rotation.

displacements to the southeast, suggesting a dextral strike-slip component on these faults. Similarly, the northwesternmost fault has a sinistral strike-slip component. Furthermore, the main first-order fault bounding the Gullfaks Sør to the west shows slip to the east-southeast, implying a sinistral strike-slip component along the east-west–striking part of the fault. Within the hanging wall of this fault, major faults are predominantly dip-slip, showing that the divergent displacement pattern within the Gullfaks Sør fault block is related to the change in fault strikes, from north-south in the northern part, to northeast-southwest in the southern part.

Note how slip may change direction along strike of some of the throughgoing faults. This change of direction is mainly a consequence of branching faults or connecting accommodation faults allowing nonuniform block movements in the hanging wall to the main fault.

RESTORATION OF THE TOP STATFJORD HORIZON, GULLFAKS FIELD

We restored more detailed maps of the top Statfjord horizon within both the Gullfaks and Gullfaks Sør fields to examine the internal deformation more closely in these areas. The top Statfjord horizon was chosen for restoration of the Gullfaks field due to the extensive erosion of the overlying Brent Group in the eastern part of the field. The fault patterns on the top Brent and top Statfjord levels, however, are similar.

Fault Block Map and Restoration

Main faults on the top Statfjord map (Figure 8a) in the Gullfaks field are north-south trending, with horizontal offset typically in the range of 250 to 500 m. These faults are second-order faults in a

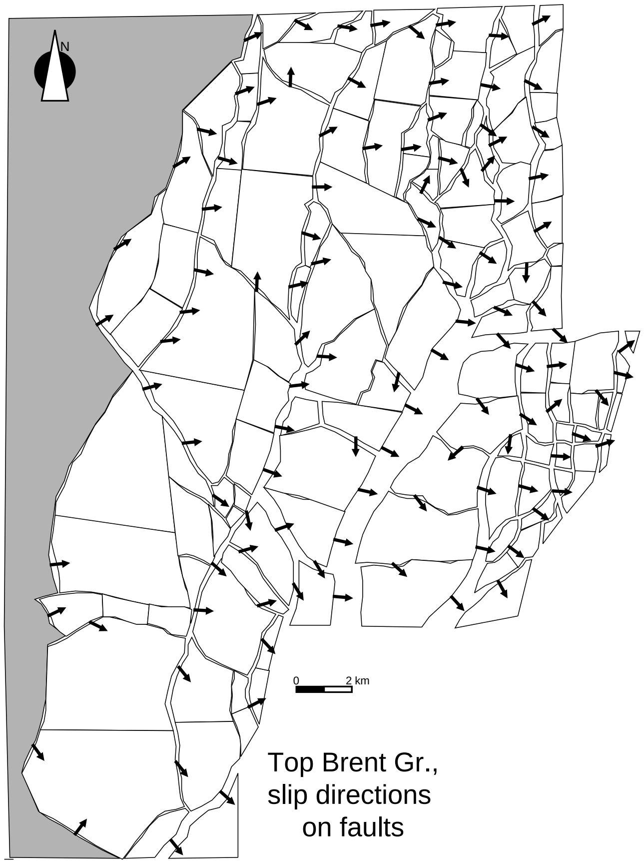

Figure 7—Direction of slip on faults as deduced from restoration of the top Brent horizon (area 1 in Figure 1). See text for discussion.

regional context. The related fault blocks are subdivided by third-order faults with horizontal offset of about 0–100 m and with variable orientation. By extrapolating fault tips and adding a few artificial discontinuity boundaries, a total of 165 blocks were defined (Figure 8a). The western boundary of the field was chosen to be stationary during deformation (gray area, Figure 8). All other external boundaries are free.

The restored block map (Figure 8b) shows a satisfactory fit, although some local gaps and overlaps remain. Comparison of the deformed (present) and restored maps shows that the area increase is 42% of the original (restored) area. The change is largest in the east-west direction (Figure 8b), but some extension also occurred in the north-south direction (i.e., slightly nonplane strain). Hence, the average extension along east-west profile lines is somewhat less than 42%, and has been found to range from about 35% (1.5 km) in the northern part through 25% (2.2 km) in the central portion to approximately 40% (1.5 km) in the south.

Fields of Finite Displacements and Rotations

Displacement vectors are slightly divergent over the Gullfaks field, ranging from east-west in the northern and northeastern parts of the area, to east-northeast–west-southwest in the southern and western part (Figure 9a), suggesting a nonplane overall strain, although not very different from plane strain. However, within the horst domain (i.e., the eastern part of the Gullfaks field), displacement vectors trend east-west and are parallel, suggesting plane strain within the horst domain. Furthermore, within the southern area, vectors are east-southeast–west-northwest oriented, but because they are subparallel, the strain can be regarded as plane in this area also.

The displacement field shows a small domain of southward displacements in the southwest. Their presence can be partly attributed to the occurrence of east-west–striking minor faults in the southwestern part of the Gullfaks field. However, their existence more likely results from the northward displacement of these blocks during the restoration to close the north-northwest–south-southeast main fault. These blocks are located at the edge of the map, and this southward displacement could thus be a boundary effect that does not reflect the actual geologic displacement. In fact, such a southward displacement has not been computed on the displacement field of the top Brent horizon where the blocks do not lie at the edge of the block map (Figure 6a).

Block rotations (Figure 9b) are small (mostly between –5 and 3°). Most rotations are clockwise except in the southwestern part of the area.

Direction of Slip on Faults

Most of the main faults are close to dip-slip according to the model (Figure 10); however, small dextral and sinistral strike-slip components do occur. Many of the small east-west–striking faults show significant sinistral strike-slip components, indicating that most small faults accommodated differential slip along the main faults during deformation.

RESTORATION OF THE TOP STATFJORD HORIZON, GULLFAKS SØR FAULT BLOCK

Similar to the Gullfaks field, the Brent Group is eroded in the eastern parts of the Gullfaks Sør fault block, and hence the Statfjord horizon has been chosen for map view restoration.

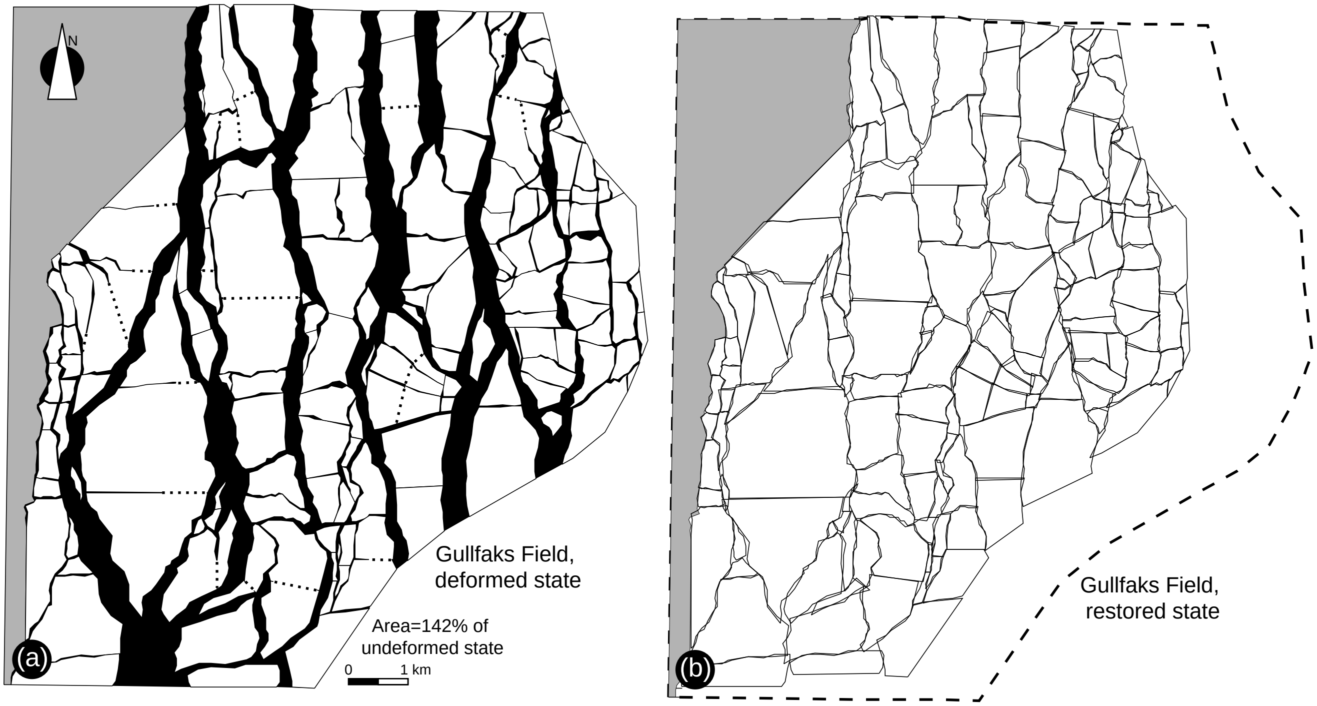

Figure 8—Fault block map for (a) the current state and (b) the restored state for the top Statfjord Formation in the Gullfaks field (area 2 in Figure 1). See Figure 6 for further explanation.

Fault Block Map and Restoration

The fault map of the Statfjord horizon in the Gullfaks Sør area is located east of the first-order fault bounding the field to the north and west (Figure 1); i.e., the map covers the hanging-wall block of this listric fault (Figure 2b). Second-order faults (of about 500 m horizontal offset) strike north-south in the northern part of the area and northeast-southwest in the south. Smaller faults (of about 50–100 m of horizontal offset) strike north-south and east-west, as well as northeast-southwest in the southern part of the area.

The fault block map of Figure 11a defines 52 blocks. We chose the western boundary of the area as a stable reference and let all other external boundaries be free to move. The restored block map (Figure 11b) shows a satisfactory fit. A few remaining gaps and overlaps can be attributed to internal block strain or erroneous seismic interpretation.

The difference in area (area dilation) between the restored and deformed states, which is an expression of strain in the horizontal plane, is about 33% of the original (restored) area. The east-west extension (line extension) is about 30% (1–1.3 km) in the northern and central part of the Gullfaks Sør structure, increasing to 40–50% (1.2–1.75 km) farther south.

Fields of Finite Displacements and Finite Rotations

Displacement vectors are divergent over the Gullfaks Sør area, ranging from east-west in the northern part of the area to southeast-northwest in the southern part (Figure 12a). This scenario is consistent with the displacement field calculated from the regional top Brent map (Figure 6a).

As for the Gullfaks field, block rotations (Figure 12b) are small (mostly between −5 and 4°). A northern domain has undergone predominantly counterclockwise rotation, and a southern domain mostly clockwise rotation, consistent with the divergent aspect of displacement vectors throughout the area.

Direction of Slip on Faults

Fault slip directions calculated from the restoration procedure (Figure 13) show a considerable spread in azimuth partly because the faults themselves show considerable variation in strike, and because most faults are close to dip-slip in the area; however, some faults are oblique slip. In particular, some of the minor east-west–striking faults show significant sinistral strike-slip components, and some faults in the central and southern part of the area show dextral strike-slip components.

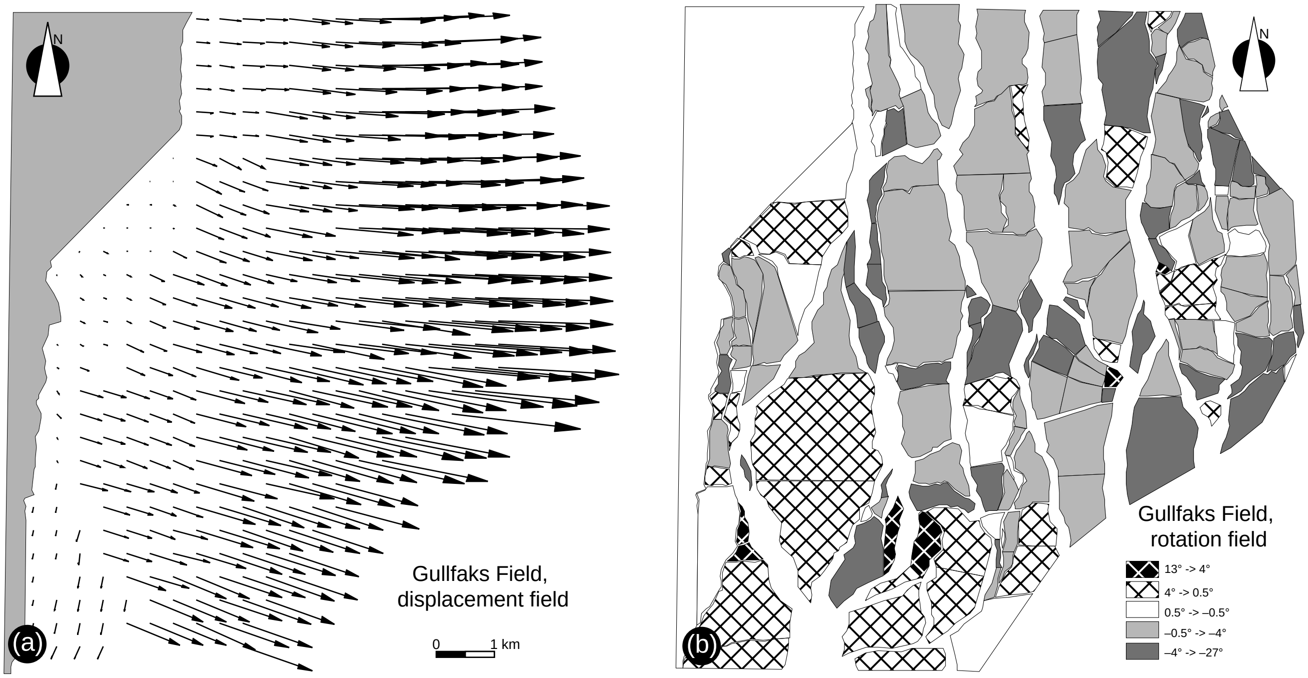

Figure 9—(a) Field of finite displacements and (b) block rotations for the top Statfjord Formation in the Gullfaks field (area 2 in Figure 1). See Figure 6 for key.

DISCUSSION

Displacement Fields

The displacement fields obtained at both regional and local scales in the larger Gullfaks area show mostly east-west directions. This verifies previous assumptions about the extension direction in the area (e.g., Speksnijder, 1987; Roberts et al., 1990); however, we did find some marked regional and local deviations from the general east-west trend, as can be seen from the general displacement field computed from the top Brent map (Figure 6a). The most pronounced deviation is the Gullfaks Sør fault block, which forms a separate domain dominated by east-southeast–west-northwest displacements. The Gullfaks Sør fault block separated from the Gullfaks fault block by a branch from the first-order fault east of the Gullfaks field (fault C in Figure 1).

The Gullfaks field (Figure 9) also shows a slightly divergent pattern. At a regional scale, this area forms a deeply eroded structural high. In general, there is a tendency for the calculated displacement pattern to diverge slightly toward perpendicular with the first-order fault east of the Gullfaks fault block (fault C in Figure 1). Although the exact reason for this pattern is not known, a thin-skinned gravitational collapse of the high eastern portion of the Gullfaks fault block may be a reasonable explanation. The detachments under the Gullfaks and Gullfaks Sør areas (Figure 2) would then either be a result of extensional collapse or provide a structural feature above which the upper part of the area could collapse gravitationally.

Many faults appear to be dip-slip, particularly north-south–trending faults. However, faults of different orientations may show a significant strike-slip component, for example along the east-west segment of the first-order fault bounding the Gullfaks Sør field to the west (fault C, Figure 1). Such strike-slip components are consistent with an overall east-west displacement direction, suggesting that the changes in slip direction are related to variations in fault orientation and not to any regional strike-slip deformation or significant block rotations (the rotations computed are small and unsystematic, and thus likely to be related to horizontal displacement gradients along faults). Knowledge of strike-slip components on faults is of interest, for example, in fault-seal analysis. Normally, only the vertical (dip-slip) displacement component is detectable from seismic data, whereas the actual displacement may be considerably larger. Because larger displacements tend to produce more fault rock material (gouge), increased displacement should result in an increased estimate of the sealing capacity of the fault.

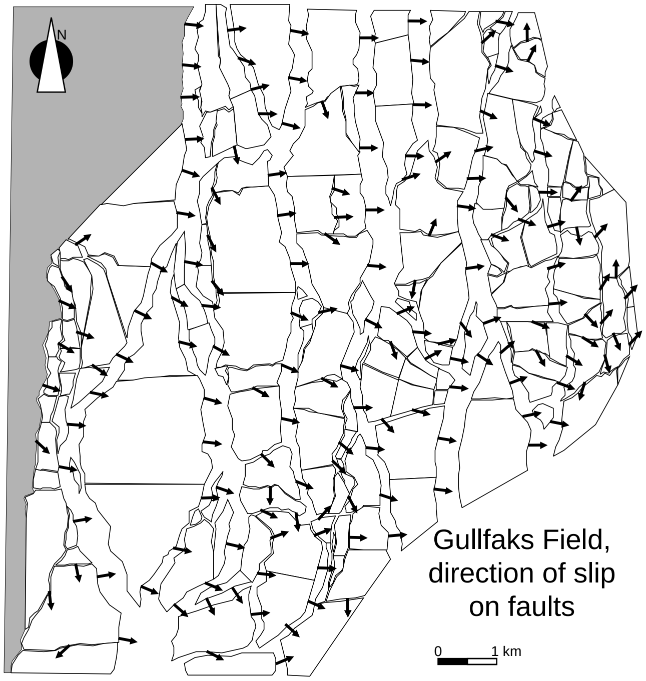

Figure 10—Direction of slip on faults as deduced from restoration of the top Statfjord Formation in the Gullfaks field (area 2 in Figure 1).

Extension and Deformation

The Gullfaks field and the Gullfaks Sør structure may be considered as two large-scale expressions of extensional collapse of the high portions of large (first-order) rotated fault blocks. For Gullfaks, a shallow-dipping detachment developed under the reservoir, linked to the second-order block-internal faults. For Gullfaks Sør, however, a large, listric fault is directly linked with the main, first-order fault east of the Gullfaks block (fault C). The listric fault developed into a large, kilometer-scale fault, and controlled the deformation within the Gullfaks Sør block.

We obtain much smaller estimates of extension for the regional map (19% of surface dilation) than for the Gullfaks field and the Gullfaks Sør structure individually (42 and 33%, respectively). This difference is in agreement with the detachment (collapse) model for the Gullfaks and Gullfaks Sør areas. The detachment model implies that the area west of fault B (Figure 1) is detached from the rest of the Gullfaks fault block, and thus could experience considerably more extension than the area to the west. Late Jurassic east-west extensions on the order of 35–40%, as seen in the Gullfaks and Gullfaks Sør areas, are unusually

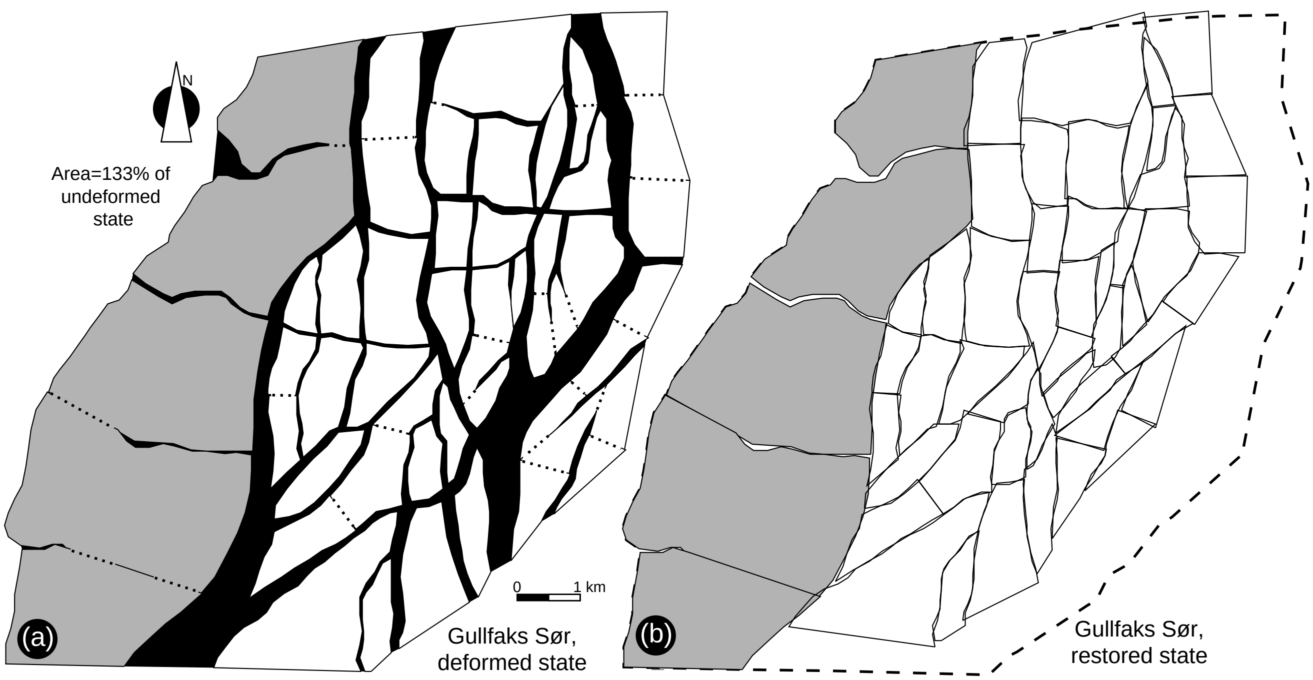

Figure 11—Fault block map for (a) the current and (b) the restored state for the Statfjord Formation map in the Gullfaks Sør area (area 3 in Figure 1). See Figure 6 for further explanation.

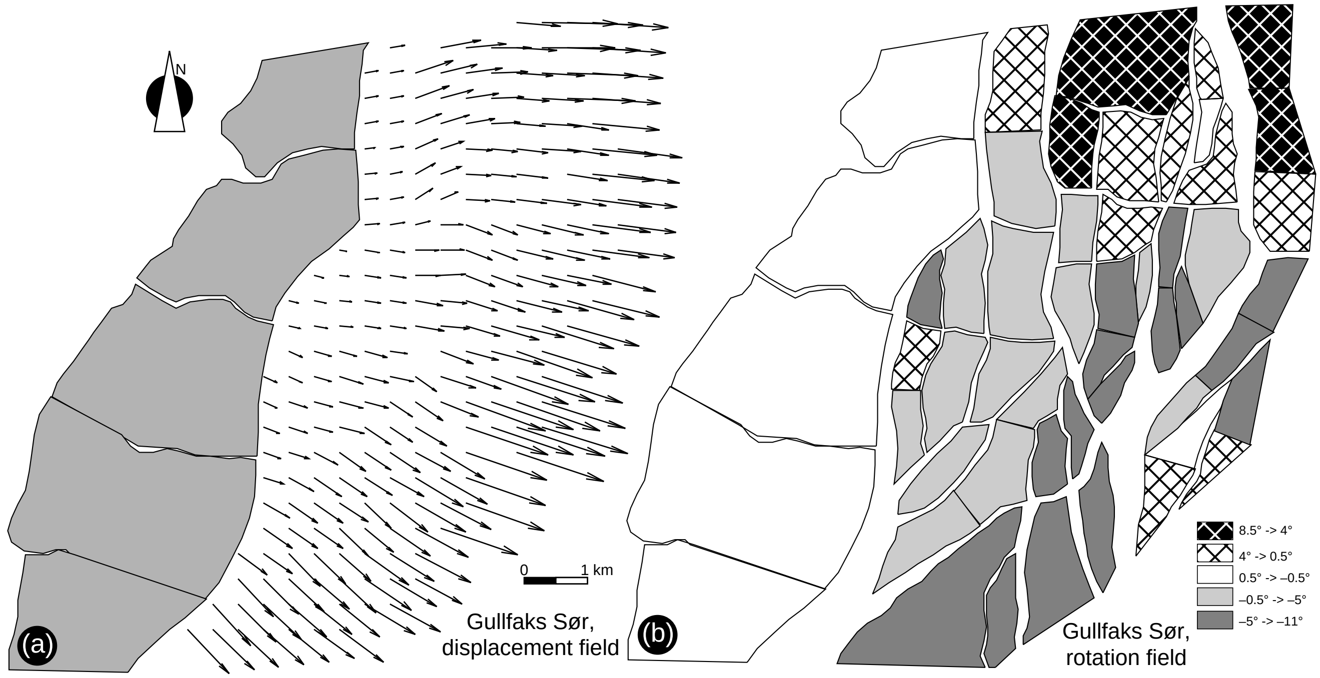

Figure 12—Field of finite (a) displacements and (b) rotations for the top Statfjord Formation in the Gullfaks Sør fault block (area 3 in Figure 1). See Figure 6 for key.

high for this part of the North Sea, where the average seismically resolvable extension related to this phase is estimated by various workers to be about 5–20% (Marsden et al., 1990; Roberts et al., 1993). However, the extension estimates rise to 30–40% within the Viking Graben east of Gullfaks.

The difference in the amount of extension computed for the Gullfaks field and the Gullfaks Sør structure may not be geologically significant. This difference is at least partly a result of the better resolution of the top Statfjord interpretation from the Gullfaks field than from the Gullfaks Sør structure; i.e., the difference may be explained by more small-scale extensional faults being included in the Gullfaks map. Because additional subseismic faults also contribute to extension in both areas, the extension estimates presented here are likely to be minimum estimates (Scholz and Cowie, 1990; Marrett and Allmendinger, 1992; Walsh and Watterson, 1992; Westaway, 1994). In addition, the Gullfaks and Gullfaks Sør fault blocks are likely to be affected by inclined internal shear deformation rather than the vertical shear assumed in the restoration model. The effect of inclined shear deformation is to stretch the fault blocks. Because this has not been accounted for in the present restoration model, the true extension is larger than the estimates presented here. The length of the true displacement vectors thus will be somewhat longer than those presented in Figures 6a, 9a, and 12a, but the displacement pattern will hardly be changed. If the internal antithetic or synthetic shear deformation acts in the direction of maximum dip of the shear plane, the effect would be to stretch the displacement pattern slightly in the shear direction. Hence, any divergent pattern would be slightly less (but still) divergent after such a correction.

Implications for Section Balancing

Section balancing normally involves the assumption of plane-strain deformation with the extension direction being parallel to the chosen section (e.g., Gibbs, 1983; Rowan and Kligfield, 1989). Furthermore, the slip directions on the faults that intersect the section should ideally be parallel to the section line. Balancing is commonly performed without detailed knowledge about the nature of the deformation in the area under consideration. Obviously, if the extension direction makes an angle to the section line, or if the strain is three-dimensional, significant errors may occur during restoration. Map view restorations provide a means of identifying and avoiding or reducing such errors. The section should be oriented parallel to the displacement direction, as imaged on displacement maps similar to that shown in Figure 6a.

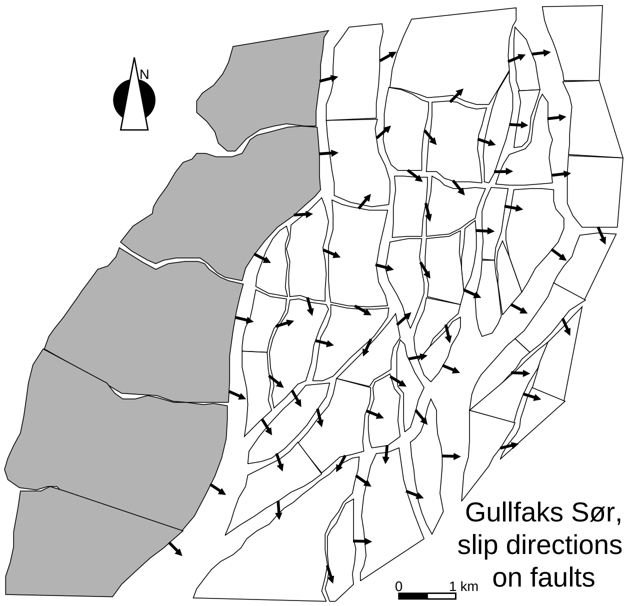

Figure 13—Direction of slip on faults as deduced from restoration of the top Statfjord Formation in the Gullfaks Sør area (area 3 in Figure 1).

This direction is not necessarily perpendicular to the main faults of an area because natural faults are generally oblique slip. If the displacement pattern is curved, the section should be segmented correspondingly. For example, a section across the southern part of Figure 1 should be oriented east-southeast–west-northwest across the Gullfaks Sør structure, and change to east-west to the west of this field. Areas of strongly divergent displacement fields or complex fault-slip patterns are not well suited for cross section balancing.

Manual restoration of a fault heave map can be performed in a relatively short amount of time. Although a fault heave map is not as accurate as the numerical procedure presented here, it provides a displacement map that would be very valuable for section balancing evaluation.

CONCLUSIONS

(1) The regional displacement pattern in the larger Gullfaks area, and particularly within the Gullfaks Sør fault block, is slightly divergent. The divergent nature of the displacement pattern may possibly reflect the influence of extensional collapse over shallow detachments of the eastern, high portions of the area.

(2) The average displacement direction is east-west.

(3) Within subdomains like the horst domain in the Gullfaks field (i.e., the northeastern part of the field), displacement vectors are almost parallel and the deformation is approximately plane strain.

(4) An abrupt break in displacement direction occurs across the first-order fault west of Gullfaks Sør (fault C, Figure 1). The break can be explained by a listric shape of the fault, where the Gullfaks Sør block deformed by hanging-wall collapse.

(5) Total extension in the horizontal plane is estimated to be 19% on average in the entire region studied (excluding the easternmost, eroded part of Gullfaks and Gullfaks Sør), but as much as 42% in the Gullfaks field and 33% in Gullfaks Sør. The high extensions in the Gullfaks field and Gullfaks Sør area are explained by extensional collapse of the eastern elevated part of a 20–25-km-wide fault block above a low-angle detachment fault.

(6) Only very minor (<5°) block rotations are calculated, giving no evidence for strike-slip motions within the area. Most of the computed rotations are related to local displacement gradients along the strike of the faults.

(7) Slip directions on faults indicate that major, second-order north-south–striking faults are dip-slip, whereas most shorter, east-west–striking faults are oblique slip. The east-west bend of the large (first-order) fault between the Gullfaks field and Gullfaks Sør (fault C, Figure 1) has strongly oblique slip (sinistral) along this segment.

(8) Map view restoration of the type demonstrated here is recommended prior to cross section balancing because map view restoration provides a description of strain (deviation from plane strain) and helps in choosing the best orientation of the cross section.

(9) The deformation in the Gullfaks area is sufficiently close to plane strain that section balancing is justified.

(10) Sections for balancing in the larger Gullfaks area should be chosen according to the displacement directions computed by the present restoration; i.e., east-west in the main Gullfaks field and east-southeast–west-northwest in the Gullfaks Sør field.

(11) Although only the vertical (dip-slip) displacement component is normally detectable from seismic data, true slip directions are calculated in the method presented in this paper. For some of the faults, the strike-slip component is larger than the dip-slip component. Assuming a relationship between sealing capacity and displacement along faults, the actual amount of slip associated with each fault can be calculated and used as an input parameter in fault-seal analyses.

REFERENCES CITED

Anderson, E. M., 1951, The dynamics of faulting: Edinburgh, Oliver and Boyd, 206 p.

Erichsen, T., M. Helle, J. Henden, and A. Rognebakke, 1987, Gullfaks, *in* A. M. Spencer, E. Holter, C. J. Campbell, S. H. Hanslien, P. Nelson, E. Nysæther, and E. Ormaasen, eds., Geology of the Norwegian oil and gas fields: London, Graham and Trotman, p. 283–286.

Færseth, R. B., T. S. Sjøblom, R. J. Steel, T. Liljedahl, B. E. Sauar, and T. Tjelland, 1995, Tectonic controls on Bathonian–Volgian syn-rift successions on the Visund fault block, northern North Sea, *in* R. J. Steel, ed., Sequence stratigraphy on the northwest European margin: Norwegian Petroleum Society (NPF) Special Publication 5, p. 325–346.

Fossen, H., 1989, Indication of transpressional tectonics in the Gullfaks oil field, northern North Sea: Marine and Petroleum Geology, v. 6, p. 22–30.

Fossen, H., and J. Hesthammer, 1994, Structural geology of the Gullfaks field, northern North Sea: Internal Statoil report no. GF/PETEK945145R, 488 p.

Fossen, H., and J. Hesthammer, in press, Structural geology of the Gullfaks field, northern North Sea, *in* M. P. Coward, ed., Structural geology in reservoir characterization and field development: Geological Society of London Special Publication.

Fossen, H., and A. Rørnes, 1996, Properties of fault populations in the Gullfaks field, northern North Sea: Journal of Structural Geology, v. 18, p. 179–190.

Gabrielsen, R. H., R. B. Færseth, R. J. Steel, S. Idil, and O. S. Kløvjan, 1990, Architectural styles of basin fill in the northern Viking Graben, *in* D. J. Blundell and A. D. Gibbs, eds., Tectonic evolution of the North Sea rifts: Oxford, Clarendon Press, p. 158–183.

Gibbs, A. D., 1983, Balanced cross-section construction from seismic sections in areas of extensional tectonics: Journal of Structural Geology, v. 5, p. 153–160.

Jackson, J. A., 1987, Active normal faults and crustal extension, *in* M. P. Coward, J. F. Dewey, and P. L. Hancock, eds., Continental extensional tectonics: Geological Society of London Special Publication 28, p. 3–17.

Karlsson, W., 1986, The Snorre, Statfjord and Gullfaks oilfields and the habitat of hydrocarbons on the Tampen Spur, offshore Norway, *in* A. M. Spencer, E. Holter, C. J. Campbell, S. H. Hanslien, P. Nelson, E. Nysæther, and E. Ormaasen, eds., Habitat of hydrocarbons in the Norwegian continental shelf: Norwegian Petroleum Society: London, Graham and Trotman, p. 181–197.

Koestler, A. G., A. G. Milnes, and A. Storli, 1992, Complex hanging-wall deformation above an extensional detachment—example: Gullfaks field, northern North Sea, *in* R. M. Larsen et al., eds., Tectonic modelling and its application to petroleum geology: NPF Special Publication 1, p. 243–251.

Marrett, R., and R. W. Allmendinger, 1992, Amount of extension on "small" faults: an example from the Viking Graben: Geology, v. 20, p. 47–50.

Marsden, G., G. Yielding, A. M. Roberts, and N. J. Kusznir, 1990, Application of a flexural cantilever simple-shear/pure shear model of continental lithosphere extension to the formation of the northern North Sea basin, *in* D. J. Blundell and A. D. Gibbs, eds., Tectonic evolution of the North Sea rifts: Oxford, Clarendon Press, p. 241–261.

Petterson, O., A. Storli, E. Ljosland, and I. Massie, 1990, The Gullfaks field: geology and reservoir development, *in* A. T. Buller et al., eds., North Sea oil and gas reservoirs—II: London, Graham and Trotman, p. 67–90.

Roberts, A. M., G. Yielding, and M. E. Badley, 1990, A kinematic model for the orthogonal opening of the Late Jurassic North Sea rift system, Denmark-Mid Norway, *in* D. J. Blundell and A. D. Gibbs, eds., Tectonic evolution of the North Sea rifts: Oxford, Clarendon Press, p. 180–199.

Roberts, A. M., G. Yielding, N. J. Kusznir, I. M. Walker, and D. Dorn-Lopez, 1993, Mesozoic extension in the North Sea: constraints from flexural backstripping, forward modelling and fault populations, *in* J. R. Parker, ed., Petroleum geology of northern Europe: Geological Society of London, p. 1123–1136.

Roberts, A. M., G. Yielding, N. J. Kusznir, I. M. Walker, and D. Dorn-Lopez, 1995, Quantitative analysis of Triassic extension in the northern Viking Graben: Geological Society of London, v. 152, p. 15–26.

Rouby, D., 1995, Restauration en carte des domaines failleés en extension. Méthode et applications. Mémoire de documents de Géosciences Rennes: Géosciences Rennes 57, 266 p.

Rouby, D., P. R. Cobbold, P. Szatmari, S. Demerican, D. Coelho, and J. A. Rici, 1993, Least-squares palinspastic restoration of regions of normal faulting—application to the Campos basin (Brazil): Tectonophysics, v. 221, p. 439–452.

Rowan, M. G., and R. Kligfield, 1989, Cross section restoration and balancing as aid to seismic interpretation in extensional terranes: AAPG Bulletin, v. 73, p. 955–966.

Sæland, G. T., and G. S. Simpson, 1982, Interpretation of 3-D data in delineating a subconformity trap in block 34/10, Norwegian North Sea: AAPG Bulletin, v. 66, p. 217–235.

Scholz, C. H., and P. A. Cowie, 1990, Determination of total strain from faulting using slip measurements: Nature, v. 356, p. 837–839.

Speksnijder, A., 1987, The structural configuration of Cormorant block IV in contact of the northern Viking Graben structural framework: Geologie en Mijnbouw, v. 65, p. 357–379.

Walsh, J. J., and J. Watterson, 1988, Dips of normal faults in British coal measures and other sedimentary sequences: Geological Society of London, v. 145, p. 859–873.

Walsh, J. J., and J. Watterson, 1992, Populations of faults and fault displacements and their effects on estimates of fault-related regional extension: Journal of Structural Geology, v. 14, p. 701–712.

Westaway, R., 1994, Quantitative analysis of populations of small faults: Journal of Structural Geology, v. 9, p. 1259–1273.

Ziegler, P. A., 1990, Tectonic and palaeogeographic development of the North Sea rift system, *in* D. J. Blundell and A. D. Gibbs, eds., Tectonic evolution of the North Sea rifts: Oxford, Clarendon Press, p. 1–36.

ABOUT THE AUTHORS

Delphine Rouby

Delphine Rouby received a Ph.D. in structural geology from the University of Rennes, France, in 1994. She is presently a research assistant in the Department of Geological and Geophysical Sciences of Princeton University. Her field of research is the growth of faults and fault networks using three-dimensional restoration.

Haakon Fossen

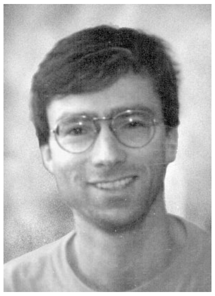

Haakon Fossen has more than 10 years of combined industrial and academic experience with focus on thrust tectonics and extensional collapse of the Caledonides, rifting, transpression, ductile shear zones, brittle deformation of rock, kinematic indicators, physical modeling, and theoretical structural geology. He holds a Cand. Mag. degree (1986) from the University of Bergen, and a Ph.D. from the University of Minnesota, Minneapolis (1992). Haakon has recently moved from Statoil, Norway, to the University of Bergen, Norway.

Peter Cobbold

Peter Cobbold received his B.Sc. degree and a Ph.D. in geology from Imperial College, London. After short periods as a lecturer at London and Leeds, he moved to Rennes, France, where he now works as a research director for the CNRS. His research interests include structural geology, tectonics, and basin development. He has been active in analog modeling, palinspastic restoration, and field work in many parts of the world, especially South Africa and central Asia.